SUPPLEMENTAL MATERIALS

DETAILED METHODS

Animals

All animal care and use procedures were approved by the University of California, Davis Institutional Animal Care and Use Committee. Experiments were performed in accordance with National Institutes of Health and institutional guidelines. All animal care and use procedures were approved by the University of California, Davis Institutional Animal Care and Use Committee. Experiments were performed in accordance with National Institutes of Health and institutional guidelines. Genetically targeted mouse models including AC_V knockout (AC_V KO)[1] and AC_{VI} knockout (AC_{VI} KO)[2] were used for the studies. The double knockout (AC_V/AC_{VI} KO) mice were generated by crossing the homozygous single KO mice. All animals were backcrossed onto the C57B1/6J mice (Jackson Laboratory) for greater than 10 generations. Wild-type (WT) littermates were used as controls. Genotype analyses were performed using PCR with specific primers for the mutant and the wild-type alleles.

Single left ventricular myocyte isolation

Single left ventricular (LV) myocytes were isolated from WT, transgenic, and KO animals at ages 10-12 week old.[3,4] The procedure was performed according to the approved UC Davis Animal Care and Use protocol. Due to the known electrophysiologic heterogeneity in various regions of the heart, we used only LV free wall cells for our electrophysiologic recordings. Briefly, mice were injected with 0.1 ml heparin (1000 units ml^{-1}) 10 min prior to heart excision, then anesthetized with pentobarbital intraperitoneally (80 mg kg^{-1}). Hearts were removed and placed in Tyrode's solution (mmol l^{-1}: NaCl 140, KCl 5.4, $MgCl_2$ 1.2, *N*-2-hydroxyethylpiperazine-*N*′-2-ethanesulphonic acid (HEPES) 5 and glucose 5, pH 7.4). The aorta was cannulated under a dissecting microscope and mounted on the Langendorff apparatus. The coronary arteries were retrogradely perfused with Tyrode's solution gassed with O_2 at 37°C for 3 min at a flow rate of ~3 ml min^{-1}. The perfusion pressure was monitored and the flow rate was adjusted to maintain perfusion pressure at ~80 mmHg. The solution was switched to Tyrode's solution containing collagenase type 2 (1 mg ml^{-1}, 330 units mg^{-1}, Worthington Biochemical Corporation). After ~12 min of enzyme perfusion, hearts were removed from the perfusion apparatus and gently teased in high-K^+ solution (mmol l^{-1}: potassium glutamate 120, KCl 20, $MgCl_2$ 1, EGTA 0.3, glucose 10 and HEPES 10, pH 7.4 with KOH). All chemicals were obtained from Sigma Chemicals (St. Louis, MO) unless stated otherwise. Cells were allowed to rest for 2 hours before use for electrophysiological recording. The isolation procedure yielded ~85% of rod-shaped myocytes with clear striation. Cardiomyocytes were used for electrophysiologic recordings within 8 hours after cell isolation.

Whole-cell patch-clamp recordings

All experiments were performed using the conventional whole-cell patch-clamp technique[5] at room temperature. In all experiments, a series resistance compensation of ≥85% was obtained. Currents were recorded using Axopatch 200B amplifier (Axon Instrument), filtered at 2 kHz using a 4-pole Bessel filter and digitized at sampling frequency of 10 kHz. Data analysis was carried out using custom-written software and commercially available PC-based spreadsheet and graphics software (MicroCal Origin version 8.6). All experiments were performed using 3 M KCl agar bridges. Cell capacitance was calculated as the ratio of total charge (the integrated area under the current transient) to the magnitude of

the pulse (20 mV). Currents were normalized to cell capacitance to obtain the current density. The series resistance was compensated electronically.

Pharmacological Interventions

For all recordings used in the study, the currents were recorded 10 minutes after whole-cell configuration was achieved for the current to stabilize. All recordings were obtained from cells with giga-ohm seals and with stable series resistance. Cells with high series resistance (> 10 MΩ) or changing series resistance were discarded. As demonstrated in the control under our recording conditions, $I_{Ca,L}$ was relatively stable with very little "rundown" of the current over a recording period of up to 30 minutes after the 10-minute waiting period. The time course of $I_{Ca,L}$ in response to pharmacological interventions was compared to the time course of $I_{Ca,L}$ in control under our recording conditions (Online Figure 2a&b).

Ca^{2+} current-voltage relations were assessed 10 minutes after the establishment of whole-cell configuration, at the beginning of application of ISO and at the end of the experiments. Current-voltage relations were constructed using a family of voltage steps of 500 ms from a holding potential of -55 mV with an interpulse interval of 2 seconds (a frequency of stimulation of 0.5 Hz). For the time course experiments, $I_{Ca,L}$ was elicited using a voltage step of 10 mV for 500 ms from a holding potential of -55 mV using an interpulse interval of 60 seconds.

For recordings using PDE inhibitors and the ß-adrenergic agonist, cells were treated first with PDE inhibitors for 30 minutes prior to the addition of ß-adrenergic agonist plus PDE inhibitors.

All chemicals were purchased from Sigma Chemical (St. Louis, MO) unless stated otherwise. The pipette solution contained (in mM) 100 CsOH, 100 ASP, 20 CsCl, 1 $MgCl_2$, 2 ATP, 0.5 GTP, 10 BAPTA, and 5 *N*-2-hydroxyethylpiperazine-*N*′-2-ethanesulphonic acid (HEPES) (pH 7.4 with HCl). The external solution contained (in mM) 140 NMG, 5 CsCl, 0.5 $MgCl_2$, 2 $CaCl_2$, 2 4-AP, 10 glucose, and 10 HEPES (pH 7.4 with MSA). Cilostamide (300 nM) and rolipram (1 μM) were used as PDE3 and PDE4 blockers, respectively, for some experiments. To separate the effects of β1-ARs and β2-AR stimulation, a selective β1 blocker (CGP-20712A methane sulfonate, 0.3 μM) or a selective β2 blocker (ICI-118,551 hydrochloride, 50 nM) were added to the external solution before the application of isoproterenol (1μM).

In some experiments, a detubulation technique consisting of an osmotic shock to internalize the t-tubules was used.[6] Specifically, cells were exposed for 20 min to formamide (1.5 M) in high K^+ solutions, followed by maintenance in high K^+ solution which contained K-Glutamine 120, KCl 20, HEPES 10, MgCl 1, EGTA 0,3, Glucose 10 . To confirm the detubulation process, confocal laser scanning microscopic images were taken after the treatment with DI-8-ANEPPS (Invitrogen, 10 μM) to stain the membrane.

Inhibitory Peptides

In a series of experiments, inhibitory peptides were developed and used at a final concentration 100 μM. Inhibitory Peptide 1 (IP1) was generated encompassing the conserved region of AC_V (AGGFGFSFRSKSAWQERGGD), Inhibitory Peptide (IP2) - scaffolding domain in CAV3 (DGVWKVSFTTFTVSKY WCYR). The corresponding control peptides (CP1 and CP2) were generated by changing aromatic amino acids to alanine, CP1 (AGGAGASARSKSAAQERGGD) and CP2 (DGVAKVSATTATVSKAACAR). Inhibitory Peptide 3 (IP3) was developed against PDE4b/PDE4d CAV3 binding domain (QVGFIDYIVHPLWETWADLV) and CP3 - (QVGAIDAIVHPLAETAADLV). Peptides were synthesized by Pi Proteomics, LLC. All peptides were added intracellular to the pipette solution.

Cell Culture and Transfection

Human Embryonic Kidney (HEK) 293 cells were cultured in DMEM supplemented with 10% fetal bovine serum and 1% penicillin/streptomycin. Cells were transfected with AC_V-HA, AC_{VI}-AU1, and

Caveolin3 constructs using Lipofectamine, LTX and PLUS reagents (Invitrogen). Cells were collected 4 days after transfection for further processing.

Western Blot Analyses

Western blot analyses were performed as previously described.[7] The protein samples were loaded in 4-20% polyacrylamide gels and SDS-PAGE was performed. Primary antibodies used in the study include anti-β-tubulin (Abcam ab6046, 1:4,000 dilution) and anti-$Ca_v1.2$ (Sigma C1603, 1:200 dilution) antibodies. Secondary antibodies include anti-rabbit IgG HRP (GE Healthcare, NA934V) and anti-mouse IgG HRP (GE Healthcare, NA931V) antibodies. Relative band intensity was determined using the Un-Scan-It gel Automated Digitizing System (Version 5.1) and normalized to β-tubulin expression (n=3, $*p \leq 0.05$).

Immunofluorescence Confocal Microscopy:

Isolated cardiac myocytes were adhered to poly-L-lysine coated coverglass and fixed in 4% paraformaldehyde (PFA). After blocking with 5% goat serum in DPBS with 0.1% triton-X to permeablize cell membranes, a primary antibody for $Ca_v1.2$ (Sigma) was incubated overnight at 4 ^oC. Alexa Fluor 555 goat anti-rabbit secondary antibody (Invitrogen) was incubated for 1 hour at room temperature. In addition, ventricular myocytes were also co-stained using polyclonal anti-caveolin-3 (Abcam ab2912, 1:1,000 dilution) antibody and monoclonal anti-α-actinin2 antibody (Sigma A7811, 1:1,000 dilution). Secondary antibodies used included Alexa Fluor 555 donkey anti-mouse antibody (Invitrogen, A31570, 1:500 dilution) and Alexa Fluor 488 chicken anti-mouse antibody (Invitrogen, A21200, 1:500 dilution). Coverslips were washed with 7 x 5 minute DPBS washes after each antibody incubation and mounted on slides with VectaShield hard set mounting medium w/DAPI (VectorBiolabs). Slides were imaged using a Zeiss confocal LSM 700 microscope and processed using the Zeiss Zen imaging software.

Real-time PCR

RNA from cardiac myocytes was isolated using the RNeasy mini isolation kit (Qiagen) according to the manufacturer's specifications. cDNA was generated from 200 ng of RNA per sample using the RT^2 First Strand kit (SA Biosciences). Quantitative RT-PCR reactions were prepared with RT^2 SYBR® Green qPCR Mastermix (SA Biosciences) and primers specific for TATA-Binding Protein (TBP) and *Cacna1c* ($Ca_v1.2$) (SA Biosciences). These reactions were run in quadruplicate in a ViiA™ 7 Real-Time PCR System (ABI) according to the manufacturer's specifications for each primer. Relative fold change was determined using the ΔΔCt method and normalized to TBP expression ($n=3$, $p \leq 0.05$).

Assessment of cAMP levels

cAMP levels in ventricular myocytes isolated from AC_V/AC_V KO and WT mice were measured using cAMP ELISA Kit (Cell Biolabs, Inc., San Diego, CA) as we have previously described.[8] Ventricular myocytes were isolated and enriched using sedimentation. The same protocol used for patch-clamp recordings was used. Specifically, cells were first incubated with PDE inhibitors for 60 minutes prior to the addition of ß-adrenergic agonist plus PDE inhibitors.

Computer modeling

Rosetta-Membrane *de novo* method[9] was used for structure prediction of caveolin. OCTOPUS server was used to define transmembrane regions within caveolin sequence.[10] We first generated 10,000 caveolin models of the transmembrane regions of caveolin followed by model clustering as described previously.[11] The center model of the largest cluster was then used for modeling of N- and C-termini of caveolin using Rosetta loop modeling method.[12] We generated10,000 full-length caveolin models followed by model clustering as described previously.[11] The center model of the largest cluster was chosen as the best model.

The WT and mutant AC_V were modeled using the PHYRE database[13]. Only the peptide segment before the first transmembrane segment was included in the modeling. The model was chosen based upon the length of the segment (minimum of 20 amino acids flanking the peptide of interest) and low e-value criteria. After both AC_V models were created, the peptides were truncated to 20 amino acids to mimic our experiments (amino acids 84-104 of the mouse WT AC_V sequence) using PyMOL (PyMOL Molecular Graphics System, Version 1.5.0.4, Schrödinger, LLC).

Molecular graphics and analyses were performed using the UCSF Chimera package (National Center for Research Resources grant 2P41RR001081, National Institute of General Medical Sciences grant 9P41GM103311).[14] The Dock 6.4 was used for the docking of the peptides[15,16]. The docking of the peptides used a rigid algorithm (the individual parts of the peptide were kept in the same orientation). The caveolin 3 peptide was treated as a receptor and the AC_V wild type and mutant peptide was treated as a ligand. The model was run six times with a range of grid from 0.1 to 10 Å to confirm the results.

Data Analyses

Where appropriate, pooled data are presented as means ± SEM. Analysis of statistical significance was performed using SigmaStat software. For multiple comparisons, one-way analysis of variance combined with Dunnett's test was used. The null hypothesis was rejected when $P < 0.05$ (two-tailed).

REFERENCES

1. Lee KW, Hong JH, Choi IY, Che Y, Lee JK, Yang SD, Song CW, Kang HS, Lee JH, Noh JS, Shin HS, Han PL. Impaired D2 dopamine receptor function in mice lacking type 5 adenylyl cyclase. *The Journal of neuroscience : the official journal of the Society for Neuroscience.* 2002;**22**:7931-7940.
2. Tang T, Gao MH, Lai NC, Firth AL, Takahashi T, Guo T, Yuan JX, Roth DM, Hammond HK. Adenylyl cyclase type 6 deletion decreases left ventricular function via impaired calcium handling. *Circulation.* 2008;**117**:61-69.
3. Li N, Timofeyev V, Tuteja D, Xu D, Lu L, Zhang Q, Zhang Z, Singapuri A, Albert TR, Rajagopal AV, Bond CT, Periasamy M, Adelman J, Chiamvimonvat N. Ablation of a Ca^{2+}-activated K^+ channel (SK2 channel) results in action potential prolongation in atrial myocytes and atrial fibrillation. *J Physiol.* 2009;**587**:1087-1100.
4. Sirish P, Lopez JE, Li N, Wong A, Timofeyev V, Young JN, Majdi M, Li RA, Chen HS, Chiamvimonvat N. MicroRNA profiling predicts a variance in the proliferative potential of cardiac progenitor cells derived from neonatal and adult murine hearts. *J Mol Cell Cardiol.* 2012;**52**:264-272.
5. Hamill OP, Marty A, Neher E, Sakmann B, Sigworth FJ. Improved patch-clamp techniques for high-resolution current recording from cells and cell-free membrane patches. *Pflugers Arch.* 1981;**391**:85-100.
6. Brette F, Komukai K, Orchard CH. Validation of formamide as a detubulation agent in isolated rat cardiac cells. *Am J Physiol Heart Circ Physiol.* 2002;**283**:H1720-1728.
7. Lu L, Zhang Q, Timofeyev V, Zhang Z, Young JN, Shin HS, Knowlton AA, Chiamvimonvat N. Molecular coupling of a Ca^{2+}-activated K^+ channel to L-type Ca^{2+} channels via alpha-actinin2. *Circ Res.* 2007;**100**:112-120.
8. Timofeyev V, Porter CA, Tuteja D, Qiu H, Li N, Tang T, Singapuri A, Han PL, Lopez JE, Hammond HK, Chiamvimonvat N. Disruption of adenylyl cyclase type V does not rescue the

phenotype of cardiac-specific overexpression of Galphaq protein-induced cardiomyopathy. *Am J Physiol Heart Circ Physiol.* 2010;**299**:H1459-1467.
9. Yarov-Yarovoy V, Schonbrun J, Baker D. Multipass membrane protein structure prediction using Rosetta. *Proteins.* 2006;**62**:1010-1025.
10. Viklund H, Elofsson A. OCTOPUS: improving topology prediction by two-track ANN-based preference scores and an extended topological grammar. *Bioinformatics.* 2008;**24**:1662-1668.
11. Bonneau R, Strauss CE, Baker D. Improving the performance of Rosetta using multiple sequence alignment information and global measures of hydrophobic core formation. *Proteins.* 2001;**43**:1-11.
12. Wang C, Bradley P, Baker D. Protein-protein docking with backbone flexibility. *J Mol Biol.* 2007;**373**:503-519.
13. Kelley LA, Sternberg MJ. Protein structure prediction on the Web: a case study using the Phyre server. *Nat Protoc.* 2009;**4**:363-371.
14. Pettersen EF, Goddard TD, Huang CC, Couch GS, Greenblatt DM, Meng EC, Ferrin TE. UCSF Chimera--a visualization system for exploratory research and analysis. *J Comput Chem.* 2004;**25**:1605-1612.
15. Moustakas DT, Lang PT, Pegg S, Pettersen E, Kuntz ID, Brooijmans N, Rizzo RC. Development and validation of a modular, extensible docking program: DOCK 5. *J Comput Aided Mol Des.* 2006;**20**:601-619.
16. Graves AP, Shivakumar DM, Boyce SE, Jacobson MP, Case DA, Shoichet BK. Rescoring docking hit lists for model cavity sites: predictions and experimental testing. J Mol Biol. 2008;377:914-934.

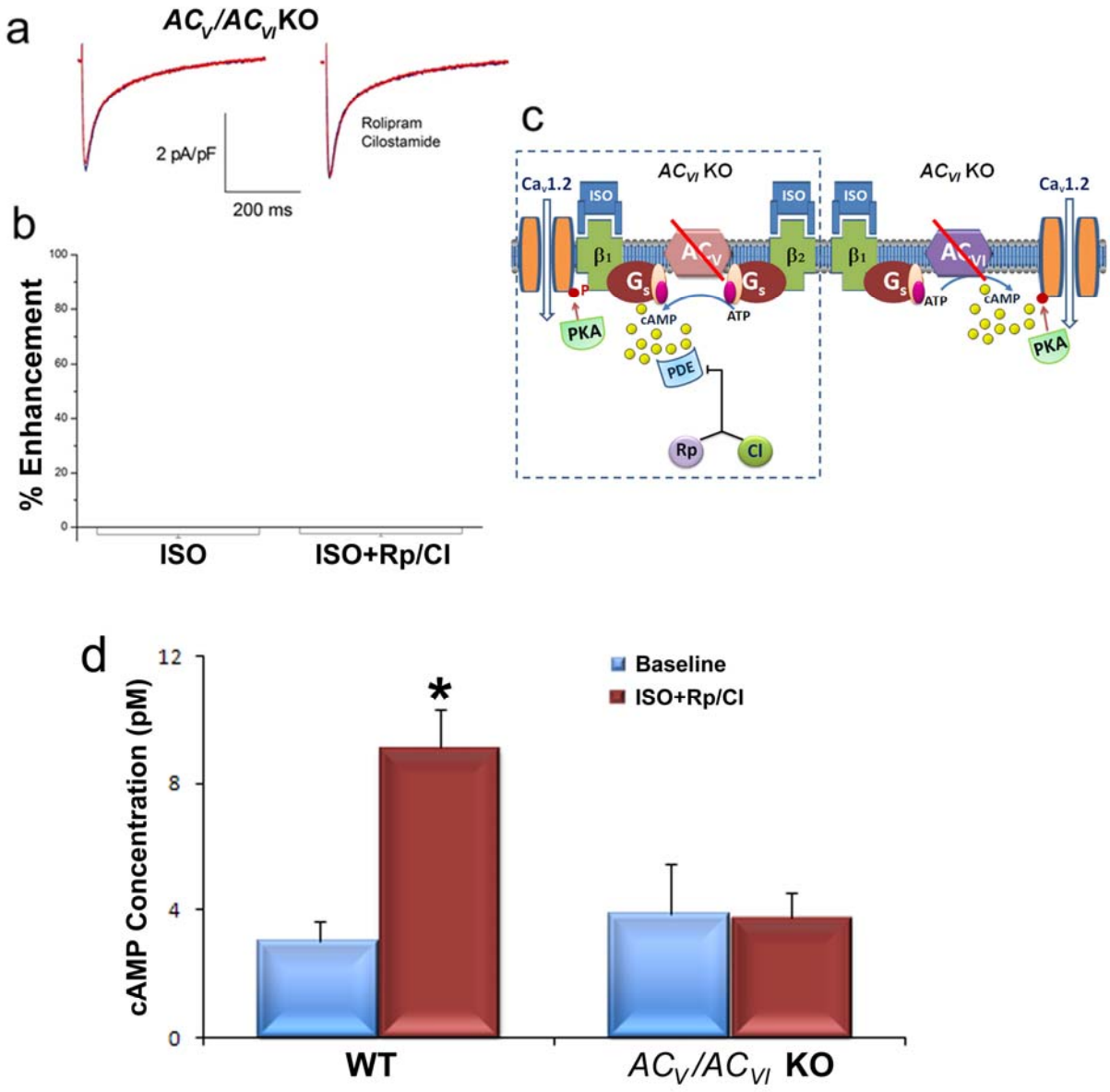

Online Figure I. AC_V and AC_{VI} represent the main ACs in ventricular cardiomyocytes.

(**a**) Representative $I_{Ca,L}$ recorded from ventricular myocytes isolated from AC_V/AC_{VI} KO mice. Current traces were elicited using a voltage step of 0 mV for 500 ms from a holding potential of -55 mV at baseline (blue) and after 20 minutes of ISO (red) without PDE blockers (left panel) and with PDE blockers (right panel). (**b**) Summary data of percent enhancement for $I_{Ca,L}$ in AC_V/AC_{VI} KO cardiomyocytes without and with PDE blockers (n=6, *P=NS*). (**c**) Schematic representation of the proposed regulation of $I_{Ca,L}$ by β_1AR and β_2AR stimulation. (d) Parallel assessment of cAMP levels in ventricular myocytes isolated from AC_V/AC_V KO and WT mice. The same protocol for patch-clamp recordings was used. Specifically, cells were first incubated with PDE inhibitors for 30 minutes prior to the addition of ISO plus PDE inhibitors for 10 minutes. Results demonstrate a lack of cAMP stimulation in AC_V/AC_V KO consistent with our patch-clamp data in (a). (*P<0.05, n = 4 samples each).

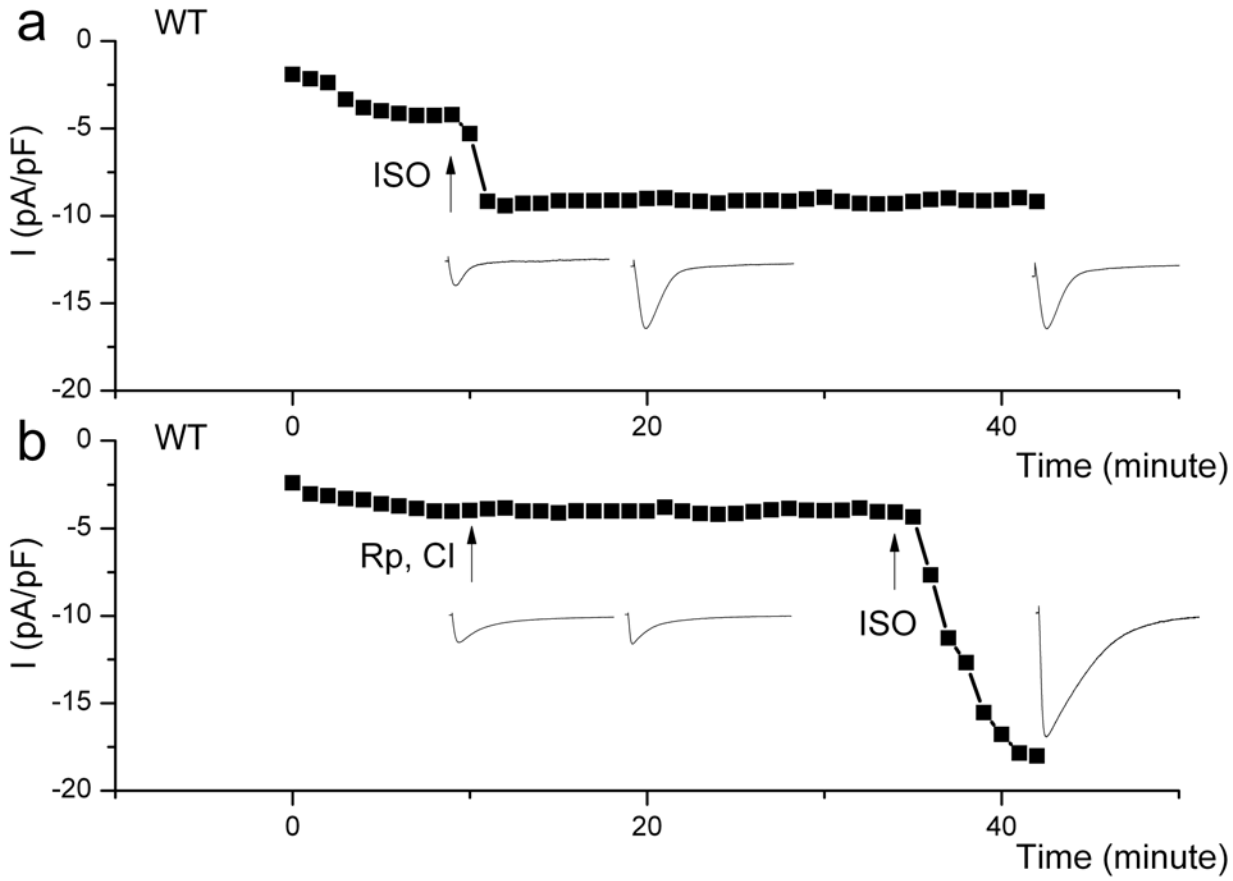

Online Figure II. Time course of $I_{Ca,L}$ recordings.

Time course of $I_{Ca,L}$ recorded from ventricular myocytes isolated from WT mice. $I_{Ca,L}$ was recorded 10 minutes after patch rupture for the current to stabilize. (a) Current traces were elicited using a voltage step of 0 mV for 500 ms from a holding potential of -55 mV at baseline and up to 30 minutes after ISO (arrow). (b) Current traces were elicited using a voltage step of 0 mV for 500 ms from a holding potential of -55 mV at baseline, after treatment with rolipram (Rp, 1 μM) and cilostamide (Cl, 300 nM, first arrow) and after ISO in the presence of rolipram and cilostamide (second arrow).

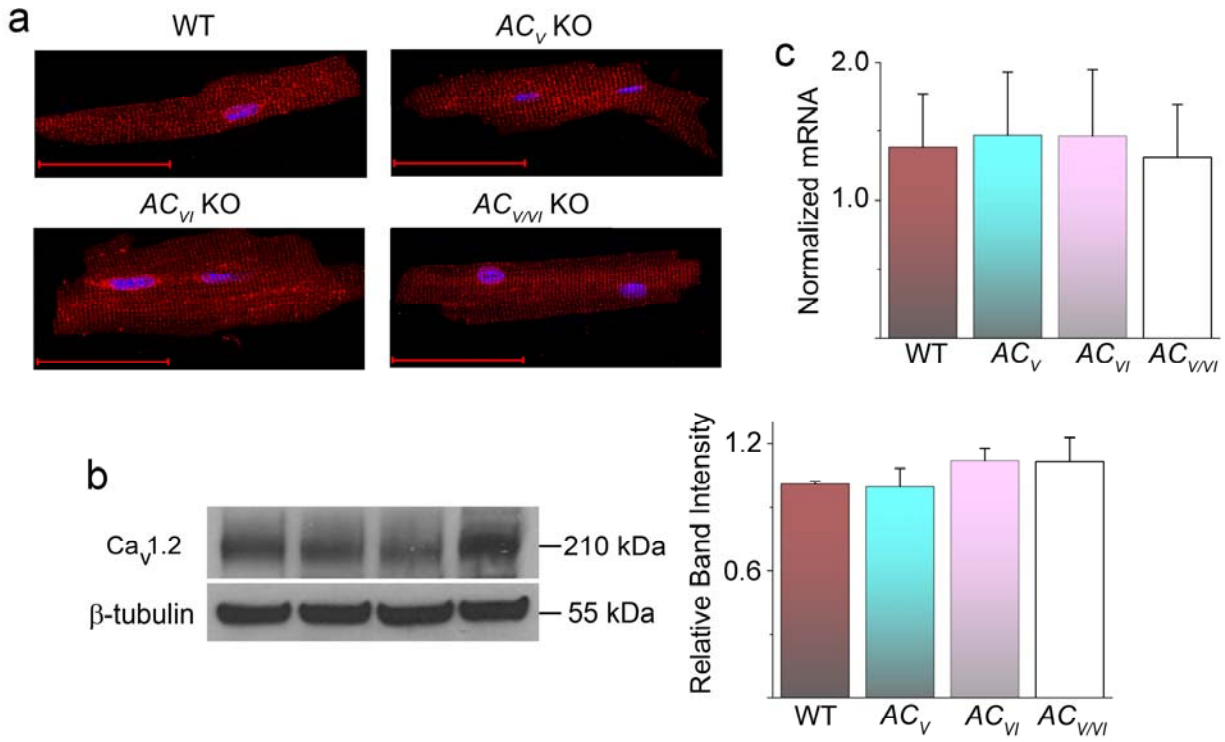

Online Figure III. The decrease in basal $I_{Ca,L}$ in AC_{VI} KO and $AC_{V/VI}$ KO was not associated with changes in the expression at the protein or transcript levels.

(**a**) Representative immunofluorescence confocal microscopic images from WT, AC_V KO, AC_{VI} KO and $AC_{V/VI}$ KO myocytes stained with anti-$Ca_v1.2$ antibodies. DAPI was used to label the nuclei. (**b**). Western blot analysis of $Ca_v1.2$ subunit from the ventricular myocytes isolated from the four groups of animals. β-tubulin was used as the loading control. Quantification is shown in the right panel (**c**) Summary data of the quantitative RT-PCR for $Ca_v1.2$ subunit. Experiments were performed in triplicate.

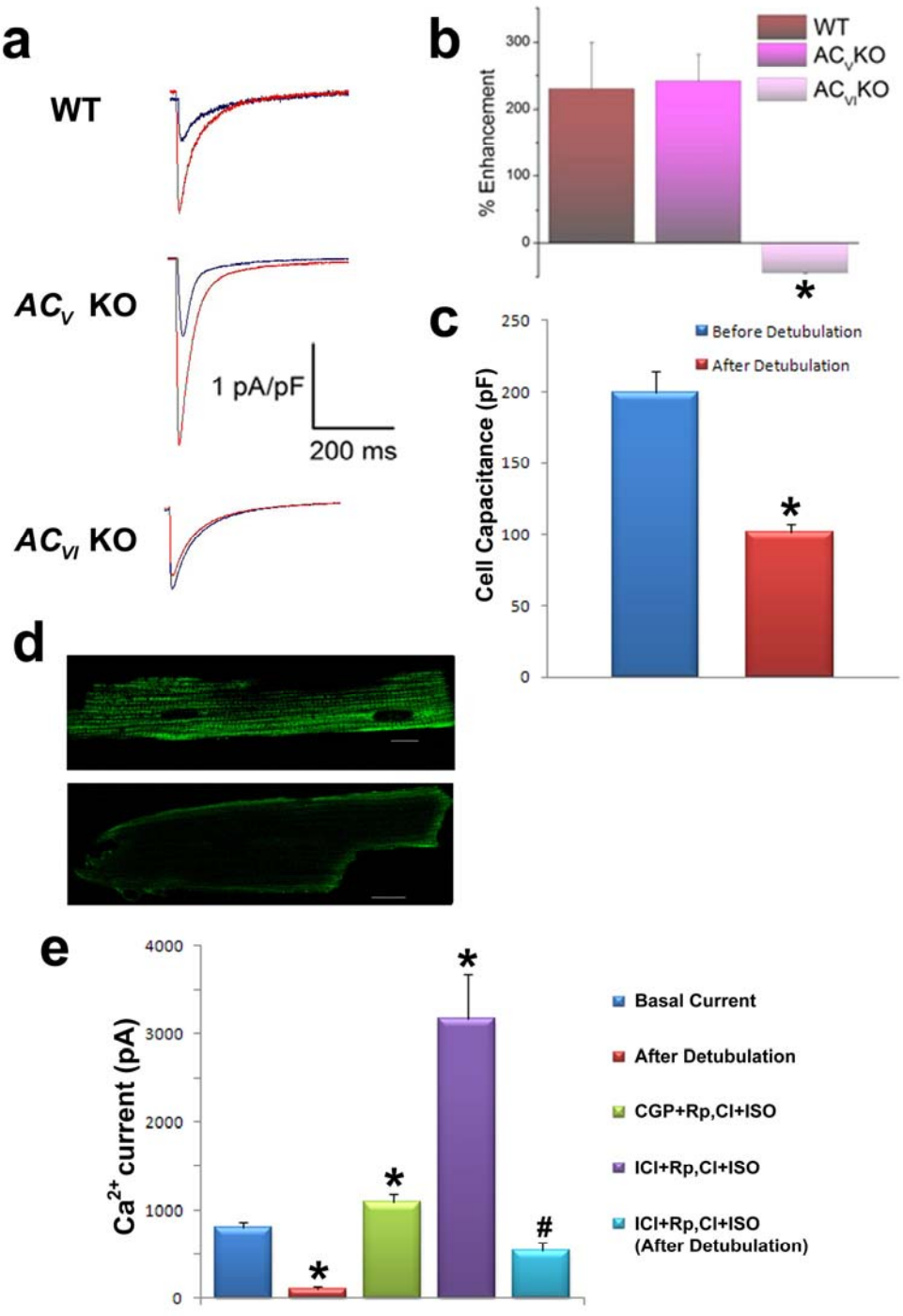

Online Figure IV. Detubulation did not alter the effects of ISO on $I_{Ca,L}$ in WT, AC_V KO, or AC_{VI} KO myocytes

(**a**) Representative $I_{Ca,L}$ recorded from ventricular myocytes isolated from WT, AC_V KO, and AC_{VI} KO mice after detubulation. Current traces were elicited using a voltage step of 0 mV for 500 ms from a holding potential of -55 mV at baseline (blue) and after 20 minutes of ISO (red). (**b**) Summary data of the

percent enhancement for $I_{Ca,L}$ in WT, AC_V KO, and AC_{VI} KO cardiomyocytes (n = 6-8 cells for each group, *P<0.05). (**c**) Comparison of the cell capacitance before and after detubulation (n = 6-8 cells for each group, *P<0.05). (**d**) Immunofluorescence confocal microscopic images of WT cardiomyocytes using DI-8-ANEPPS before (top panel) and after detubulation (bottom panel). Notice the disappearance of the striated pattern after detubulation. (e) Amplitude of $I_{Ca,L}$ elicited at 0 mV from a holding potential of -55 mV from WT ventricular myocytes before and after detubulation demonstrating a significant decrease in $I_{Ca,L}$ after detubulation (n= 6 for each group). In addition, amplitude of $I_{Ca,L}$ from WT ventricular myocytes treated with CGP-20712A, rolipram (Rp), cilostamide (Cl) and ISO. (n=6 for each group, *P<0.05 compared to basal current). The last two bars show amplitude of $I_{Ca,L}$ treated with ICI-118,551, rolipram, cilostamide and ISO in WT ventricular myocytes with and without detubulation (n=6 for each group, #P<0.05 comparing the current amplitude with and without detubulation).

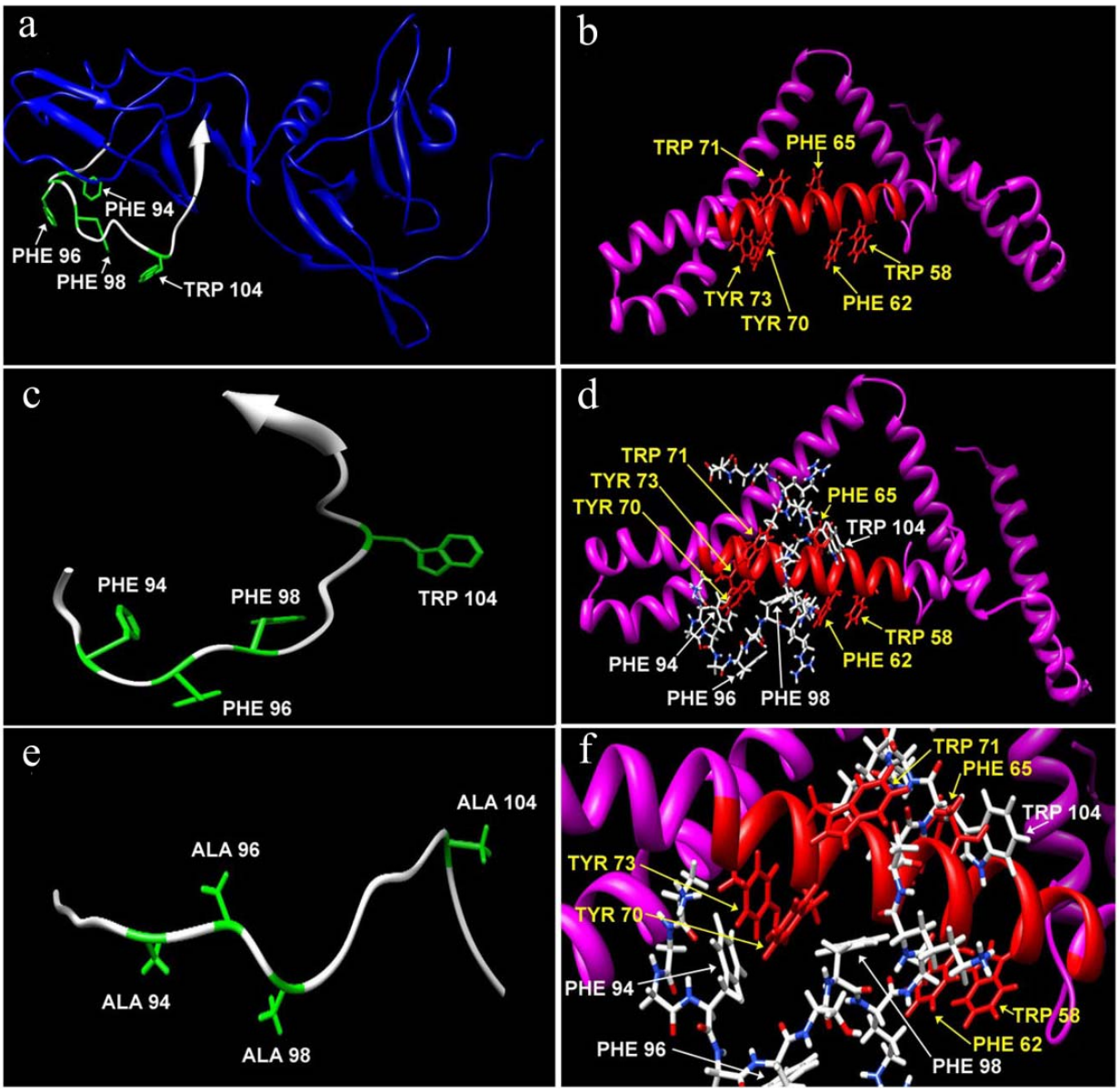

Online Figure V. Molecular modeling demonstrates the critical roles of the aromatic amino acid residues (PHE 94, 96, 98, and TRP 104) within the N terminus of AC_V isoform docked to the caveolin-3 scaffolding domain.

(**a**) The N-terminus of AC_V is shown in blue, while the predicted caveolin-3-binding domain is shown in white. The critical aromatic amino acids for the binding to the caveolin-3 scaffolding domain are shown in green using stick representation. (**b**) The N terminus of caveolin-3 is shown in magenta with the scaffolding domain shown in red. The aromatic amino acids of caveolin-3 scaffolding domain are shown using stick representation. (**c**) The putative caveolin-3 binding domain from AC_V which was used for the docking experiment. (**d**) The two peptides from b and c are docked utilizing a "site-specific docking algorithm". (**e**) The aromatic amino acid residues within the putative caveolin-binding domain from AC_V are replaced by alanine. (**f**) Two peptides as in **d** with magnified docking area, oriented for better visualization of the aromatic amino acid residues.

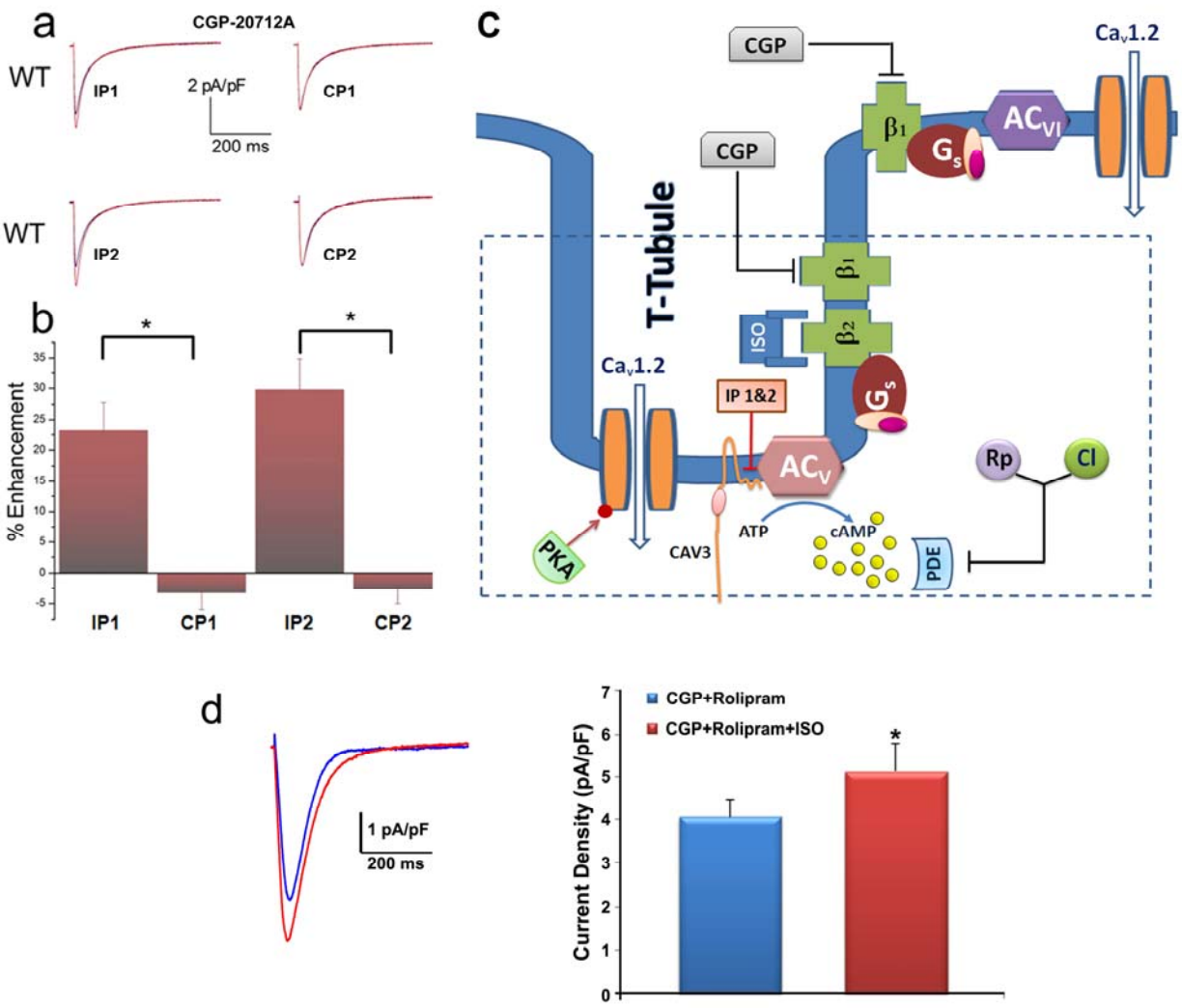

Online Figure VI. Disruption of caveolin binding or scaffolding domains results in β_2AR stimulated enhancement of $I_{Ca,L}$ in WT mice.

(**a**) Representative $I_{Ca,L}$ recorded from ventricular myocytes isolated from WT mice. Current traces were elicited using a voltage step of 0 mV for 500 ms from a holding potential of -55 mV at baseline (blue) and after 20 minutes of ISO (red) in the presence of a β1-AR blocker (CGP-20712A, CGP). Currents were recorded in the presence of the inhibitory peptides (IP1 or IP2, left panels) compared to the control peptides (CP1 or CP2, right panels). (**b**) Summary data of the percent enhancement for $I_{Ca,L}$ in the presence of inhibitory peptides (IP1 and IP2) compared to control peptides (CP1 and CP2). (**c**) Schematic representation of the experimental results which suggest a caveolin binding domain on N-terminus of the AC_V isoform. Caveolin 3 interacts and anchors the AC_V isoform within the t-tubules of the cardiac myocytes. A pink ellipse represents the caveolin scaffolding domain. (**d**) Representative $I_{Ca,L}$ recorded from ventricular myocytes isolated from WT mice. Current traces were elicited using a voltage step of 0 mV for 500 ms from a holding potential of -55 mV at baseline (blue) and after 20 minutes of ISO (red) in the presence of a β1-AR blocker (CGP-20712A, CGP) and PDE4 blocker (Rolipram). Summary data of the $I_{Ca,L}$ density before and after ISO. N=4 for each group, *P<0.05.

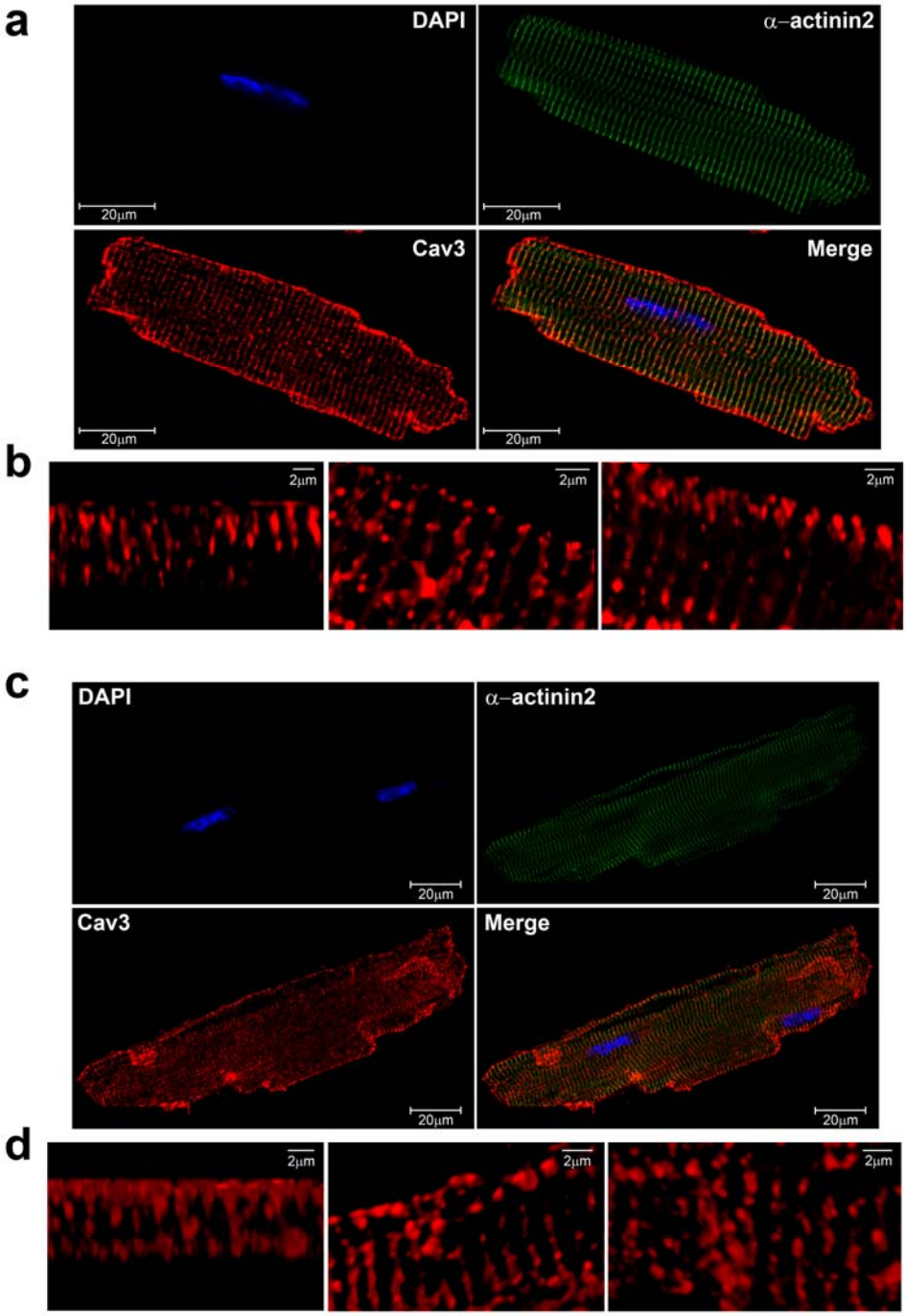

Online Figure VII. Immunofluorescence confocal microscopic images of ventricular myocytes before and after detubulation.

Representative immunofluorescence confocal microscopic images from WT ventricular myocytes before (**a,b**) and after (**c, d**) detubulation showing caveolin 3 and α-actinin2 staining along the t-tubules. (**b, d**) Images obtained before and after detubulation using 3D reconstruction from multiple Z-stacked imaging showing caveolin 3 staining along the t-tubules. DAPI was used to stain the nuclei. Merged images are

shown in the right lower corners in **a** and **c** (Merge). Please also see movies for the 3D animation in Online Movie Files.